Active Compensation Technique for Converter-Fed AC Microgrids

Bharathikannan S, Angalaeswari S

***Abstract*— The energy sector is moving towards extensive use of power electronic (PE) converters to interface distributed generation (DG) units and modern converter interfaced loads (CILs). Therefore, the conventional distribution-grid is gradually transformed into a multi-stage Power electronic converter-dominated network. However, interaction dynamics among equivalent source and load converters may adversely influence the overall voltage profile and Power factor even if each converter stage is inherently functional and stable. The STATCOM, DVR, UPS and active power conditioner are only useful for compensating a particular type of power quality problems and therefore, it has become necessary to develop a new kind of Unified Series-Shunt Compensator (USSC) which can mitigate a wider range of power quality problems. A new effort has been taken to maintain these problems without using FACTS devices. This thesis addresses interaction dynamics in emerging PE distribution systems by using small-signal linearization to derive equivalent input/output admittance models of typical Power Electronics converters. Active compensators are designed to maintain the system Voltage profile and Power factor. Theoretical analysis and extensive simulation results are presented to validate the developed models and the proposed active compensators.**

***Index Terms*— Dynamic Controllers, Active damping, microgrids, distributed generation (DG), Wind Energy.**

I. INTRODUCTION

Due to increased concerns on the availability of the conventional energy resources, distributed generation (DG) concept is adopted with high penetration of renewable energy resources to the distribution system [1]. Fig. 1 shows a schematic of a micro-grid system with typical modern loads. Typical DG units and the majority of modern loads are interfaced to the utility grid by power electronic converters for better controllability, reliability and efficiency. Several modern loads, such as motor drives, induction heating, and electric vehicles, will be interfaced via power electronic converters [2]. With the expansion of microgrids, a multi converter system with converter-interfaced-loads (CIL) and generators is created. As Wind energy has matured to a level of development where it is ready to become a generally accepted utility generation technology. Wind-turbine technology has undergone a dramatic transformation during the last 15 years, developing from a fringe science in the 1970s to the wind turbine of the 2000s using the latest in power electronics, aerodynamics, and mechanical drive train designs. In the last five years, the world wind-turbine market has been growing at over 30% a year, and wind power is playing an increasingly important role in electricity generation, especially in countries such as Germany and Spain. The legislation in both countries favors the continuing growth of installed capacity. Wind power is quite different from the conventional electricity generation with synchronous generators. a result, the distribution system is transformed to a large scale converter-fed network.

In advanced power electronic interfaces, controllers are adopted to effectively satisfy the load/generation performance requirements via tight regulation of the controlled variables. However, it has been found that a tightly regulated converter yields as a negative input impedance in the small signal sense, which reduces overall stability margin. Due to the negative impedance effect, when the terminal voltage increases / decreases, the drawn current decreases/increases. Equivalently, this behavior is represented by a constant power (CP) operation [3]–[14]. CP operation has been addressed for the tightly regulated power electronic dc-dc converters as in [3]–[5] and tightly regulated motor drive applications [6]–[8].

The compensation for the tightly regulated (or CP) effect depends on either reshaping the load impedance [3]–[5] or the source impedance [6], [7] to meet the Nyquist admittance ratio criterion [10], [11]. A multi-voltage-controlled converter system with equivalent source and load impedance is stable if the ratio of the source to the load impedance is less than unity [11].

Compensation methods for CP operation in dc micro-grid are presented in [13]. It is shown that active damping compensation is the most preferred method in DG applications to overcome such types of interaction dynamics as compared to passive techniques [12]. In [3], [13], a linear active damping method is realized by using the inductor current of the converter filter. In [4], [13], nonlinear controllers are applied to dc-dc converters operating in continuous conduction mode and loaded by CP load.

However, the complexity of the nonlinear controller makes it less attractive. Another active damping method for a voltage-source rectifier (VSR) loaded by a CIL is reported in [14]. A switched control strategy is adopted to adaptively change the voltage controller gains to preserve the system stability by reshaping the source impedance. This technique, however, demands strict information on the load profile and the design process is load-dependent.

Manuscript received May 02, 2014.

Bharathikannan S, Department Of Electrical and Electronics Engineering, Valliammai Engineering College, Chennai, India, +91 8939009793,

Angalaeswari S, Department Of Electrical and Electronics Engineering, Valliammai Engineering College, Chennai, India, +91 9841812993,

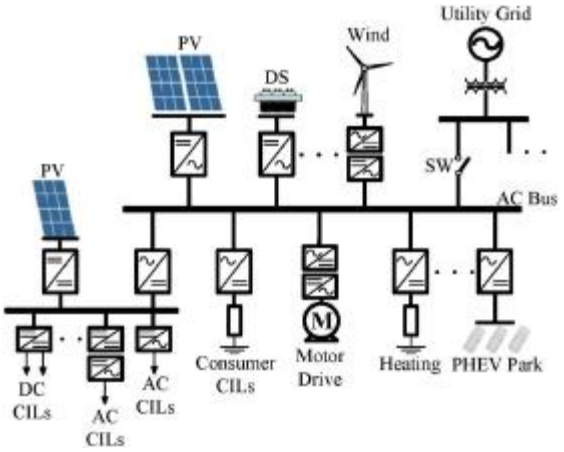

Fig. 1 Hybrid micro-grid systems

In spite of the importance of ac microgrids, all active compensation methods reported in the literature focus on the stabilization of CILs in dc-dc converters and VSRs. To the authors' knowledge, the influence of CILs on the ac micro-grid stability has been only addressed in [15]. With CP operation, it is concluded that the system stability cannot be preserved by only tuning the current and voltage controllers.

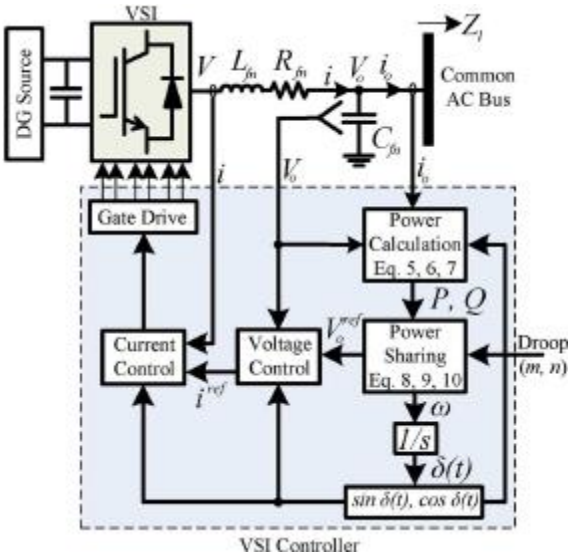

Fig. 2 Power and control structure of one DG unit interfaced by VSI in ac micro-grid

The reshaping techniques are achieved passively by adding additional resistive load parallel to the aggregated CIL so that the overall load impedance satisfies the Nyquist stability criterion. However, this approach adds restrictive conditions on the loads that can be supplied from the micro-grid, which opposes the "plug-and-play" requirements. Moreover, the penetration level of resistive load sharing decreases as compared to expected CIL penetration; therefore, the natural damping of resistive loads might not be sufficient to mitigate the effect of the CP operation.

Interaction dynamics between DG converters and CILs becomes more significant in isolated ac microgrids. In this mode, the aggregated source impedance of DG units increases, which might violate the Nyquist stability criterion. However, if the same CILs are supplied in grid-connected mode, stability margins can be remarkably improved as the aggregated source impedance of DG units and the grid decreases significantly due to the relatively large stiffness of the grid as compared to DG units.

This paper addresses ac micro-grid voltage unbalance under high penetration of tightly regulated CILs; and proposes three active damping methods depending on reshaping the VSI source impedance by injecting active damping signals to the voltage-oriented VSI control structure. Procedure for Paper Submission

II. ADMITTANCE-BASED MODELING OF TYPICAL AC MICROGRID SOURCES AND CILS

A. Modeling of VSI-Based DG Interface

Fig. 2 shows a VSI as an interface for a DG unit in ac micro-grid. Three control loops are utilized; namely they are the the power sharing, voltage, and current controllers [13], [14]. As shown in Fig. 2, the power sharing controller is used to generate the local magnitude and angle of the reference output voltage according to the droop coefficients to emulate a conventional synchronous generator. The voltage controller is used to synthesize the reference value of the inverter output current. Finally, the current controller is adopted to generate the reference input voltage command for the VSI; hence the inverter duty ratio can be determined. The controller structure is synthesized in the sense of the voltage oriented control framework. The current and voltage dynamics of the power circuits are modeled in the d-q frame that rotates synchronously with the inverter output voltage angular speed ω by:

$$V_d - V_{od} = I_d (R_f + sL_f) - \omega L_f I_q \quad (1)$$

$$V_q - V_{oq} = I_q (R_f + sL_f) + \omega L_f I_d \quad (2)$$

$$I_d - I_{od} = (sC_f + Y) V_{od} - \omega V_{oq} C_f \quad (3)$$

$$I_q - I_{oq} = (sC_f + Y) V_{oq} - \omega V_{od} C_f \quad (4)$$

Where Y is the penetrated direct resistive load to the common ac-bus and is initially set to zero (passive damping effect); V_d ,V_q , I_d and I_q are the d-q axis inverter output voltages and currents; V_{od} , V_{oq} , I_{od} and I_{oq} are the d-q axis load voltages and currents; R_f , L_f and C_f are the per-phase resistance, inductance and capacitance of the LC filter, respectively, and ?is the Laplace operator.

In the d-q synchronous reference frame, the instantaneous active (P) and reactive (q) power delivered to the ac common bus are given by:

$$p = 1.5(V_{od} I_{od} + V_{oq} I_{oq}) \quad (5)$$

$$q = 1.5(V_{od} I_{oq} + V_{oq} I_{od}) \quad (6)$$

The average active (P) and reactive (Q) powers that correspond to the fundamental components are obtained by a low-pass filter (LPF) with a cut-off frequency to achieve high power quality injection; therefore,

$$P = \omega_p \frac{p}{s+\omega_p}, \; Q = \omega_p \frac{q}{s+\omega_p} \quad (7)$$

Virtual droop characteristics are emulated in paralleled inverter systems to efficiently share the active and reactive power for the common load by introducing the following droops in the fundamental voltage frequency and magnitude of the load voltage

$$\omega = \omega^* - mP \quad (8)$$

$$V_{od}^{ref} = V_{od}^* - nQ \quad (9)$$

m and n are calculated as follows:

$$m = (\omega_{max} - \omega_{min})/P_{max} \quad (10)$$

$$n = (V_{od,max} - V_{od,min})/Q_{max} \quad (11)$$

III. VSI AS A CIL IN AC MICRO-GRIDS

This section introduces the VSR as a CIL in ac micro-grid applications. Based on small-signal linearization and admittance-based analysis, the input admittance of VSR is obtained. Active stabilization and reshaping techniques are also provided. The proposed solutions are evaluated under Matlab/Simulink platform with a complete ac micro-grid model.

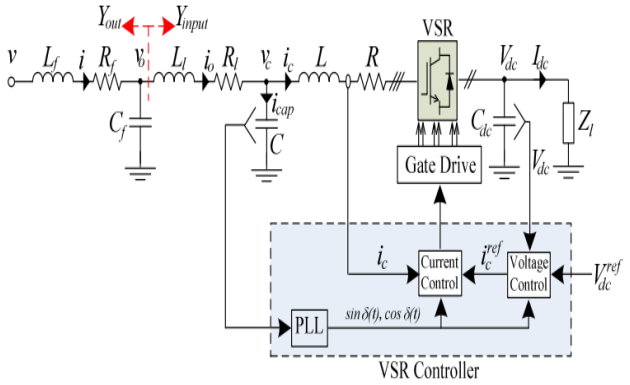

Fig. 3 Power and control structure of a VSR

Fig. 3 shows a schematic diagram of a VSR. Using the two-phase d- q synchronous reference frame that rotates by angular frequency at dedicated by a phase-looked loop (PLL), the large-signal model of VSR power circuit can be given by [11], [12]:

$$V_{cd} = I_{cd}(R + sL) - \omega L I_{cq} + D_d V_{dc} \quad (12)$$

$$V_{cq} = I_{cq}(R + sL) + \omega L I_{cd} + D_q V_{dc} \quad (13)$$

$$V_{od} = I_{od}(R_l + sL_l) - \omega L_l I_{oq} + V_{cd} \quad (14)$$

$$V_{oq} = I_{oq}(R_l + sL_l) + \omega L_l I_{od} + V_{cq} \quad (15)$$

where R_l, L_l and R, L are the per phase equivalent resistance and inductance of the distribution line and the input ac filter of the VSR, Z_l is the terminated load at the dc-side of the VSR with a dc-link voltage (V_{dc}) and input dc current I_{dc}); R_f, L_f and C_f are the output ac filter parameters of the source-side which can be a VSI [Fig. 3]; I_{cd}, I_{cq} are the d-q components of the rectifier input ac current (I_c); I_{od}, I_{oq} are the d-q components of I_o; while V_{cd}, V_{cq} and V_{od}, V_{oq} are the d-q components of the ac voltages respectively; D_d and D_q are the rectifier duty ratios in d-q frame and are determined by the control topology.

An outer PI dc voltage controller is used for dc voltage tracking and regulation, whereas an inner PI current controller is used for voltage orientation mechanism at a unity power factor by setting the quadrature component of the input ac current to zero. The mathematical model for the dc voltage controller is given by:

$$I_{cd}^{ref} = (V_{dc}^{ref} - V_{dc})G_{vdc}(s) \quad (16)$$

where it generates the d-axis component of the VSR reference current I_{cd}^{ref}. The current controller synthesizes the duty ratios in the d-q frame which are used to generate the controlled signals of the IGBT switches.

IV. PROPOSED ACTIVE COMPENSATORS

Three active compensation techniques are investigated to actively reshape the source admittance of the interfacing inverter to meet the Nyquist ratio criterion, and accordingly the stability conditions at different micro-grid loading conditions

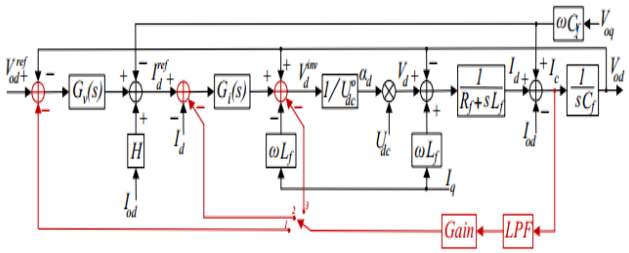

Fig. 4 Proposed active compensators. (1) RLV compensator. (2) RIC compensator. (3) RIV compensator

A. Reference-Load-Voltage (RlV) Compensator

The compensator signal is applied to the selector "1" in Fig. 4. The output load voltage V_{od} is virtually modulated by the compensator signal to embed a virtual resistive voltage component in the output voltage that is proportional to the capacitor current. This compensator modifies the actively reduce the source admittance of the VSI as follows:

$$I_d^{ref} = \left(V_{od}^{ref} - (1 + N_1(s))\, V_{od}^{ref}\right)G_v(S) - \omega C_f V_{oq} + HI_{od} \quad (17)$$

Where $N_1(s)$ is the RLV compensator transfer function and is given by:

$$N_n(s) = \frac{sK_n\omega_n C_f}{s+\omega_n}, n = 1 \quad (18)$$

With the RLV compensator, the small-signal source admittance of the VSI is given by (19).

$$\frac{\Delta I_{od}}{\Delta V_{od}} = \frac{\alpha_5 s^5 + \alpha_4 s^4 + \alpha_3 s^3 + \alpha_2 s^2 + \alpha_1 s^1 + \alpha_0}{-L_f s^4 + \left(K_{ip}^{(H-1)} - R_f - \omega_1 L_f\right)s^3 + \left((H-1)(\omega_1 K_{ip} + K_{ii}) - \omega_1 R_f\right)s^3 + \omega_1 K_{ii}(H-1)s} \quad (19)$$

$$\alpha_5 = L_f C_f$$

$$\alpha_4 = C_f(R_f + \omega_1 L_f + K_{ip})$$

$$\alpha_3 = C_f\left(R_f\,\omega_1 + K_{ii} + \omega_1 K_{ip}\left(1 + K_1 K_{vp}\right)\right) + K_{ip}K_{vp})$$

$$\alpha_2 = \omega_1 C_f\left(K_{ii} + K_1\left(K_{ip}K_{vp} + K_{ip}K_{vi}\right)\right) + K_{ip}K_{vi} + K_{ii}K_{vp} + \omega_1 K_{ip}K_{vp}$$

$$\alpha_1 = (1 + C_f K_1 \omega_1) K_{ii} K_{vi} + \omega_1 (K_{ii} K_{vp} + K_{ip} K_{vi})$$

$$\alpha_0 = \omega_1 K_{ii} K_{vi}$$

The admittance in (19) is obtained to investigate the effect of the compensator on the admittance ratio criterion. Further, to assess the DG interface stability with the RLV compensator and at different penetration levels of CILs, the characteristic equation that describes the system stability is obtained as the denominator of the following transfer function.

$$\frac{\Delta I_{od}}{\Delta V_{od}} = \frac{\left(V_d^0 / U_{dc}^0\right)(s+\omega_1)s^2}{a_5 s^5 + a_4 s^4 + a_3 s^3 + a_2 s^2 + a_1 s^1 + a_0}$$

(20)

B. *Reference-Inverter-Current (RIC) Compensator*

The compensator signal is applied to the selector "2" in Fig. 4. As shown, I_d is virtually increased by the injected compensator signal. This compensator gives,

$$V_d^{ref} = (I_d^{ref} - I_d - N_2(s)\, V_{od})\, G_i(S) - \omega L_f I_q + V_{od}$$

(21)

Where $N_2(s)$ is the RIC compensator transfer function and is given by (4.19) with n =2. The small-signal source admittance is derived when the RIC is applied as follows.

$$\frac{\Delta I_{od}}{\Delta V_{od}} = \frac{\beta_5 s^5 + \beta_4 s^4 + \beta_3 s^3 + \beta_2 s^2 + \beta_1 s^1 + \beta_0}{-L_f s^4 + \begin{pmatrix} K_{ip}(H-1) \\ -R_f - \omega_2 L_f \end{pmatrix} s^3 + \begin{pmatrix} (H-1) \\ (\omega_2 K_{ip} + K_{ii}) \\ -\omega_2 R_f \end{pmatrix} s^2 + \omega_2 K_{ii}(H-1)s}$$

(22)

$$\beta_5 = L_f C_f$$
$$\beta_4 = C_f(R_f + \omega_2 L_f + K_{ip})$$
$$\beta_3 = C_f\left(R_f\, \omega_2 + K_{ii} + \omega_2 K_{ip}(1 + K_2)\right) + K_{ip} K_{vp}$$
$$\beta_2 = \omega_2 C_f K_{ii}\left((1 + K_2)\right) K_{ip} K_{vi} + K_{ii} K_{vp} + \omega_2 K_{ip} K_{vp}$$
$$\beta_1 = K_{ip} K_{vi} + \omega_2 (K_{ii} K_{vp} + K_{ip} K_{vi})$$
$$\beta_0 = \omega_2 K_{ii} K_{vi}$$

C. *Reference-Inverter-Voltage (RIV) Compensator*

As shown in Fig. 4 with the selector at position "3", the RIV compensator modifies the direct component of the reference inverter voltage by injecting the active compensation signal. The injected reference inverter voltage is proportional to the capacitor current, and accordingly a virtual damping resistor is yielded. The modified small-signal source admittance is shown in (4.27).

$$\frac{\Delta I_{od}}{\Delta V_{od}} = \frac{y_5 s^5 + y_4 s^4 + y_3 s^3 + y_2 s^2 + y_1 s + y_0}{-L_f s^4 + \begin{pmatrix} K_{ip}^{(H-1)} \\ -R_f - \omega_1 L_f \end{pmatrix} s^3 + \begin{pmatrix} (H-1) \\ (\omega_1 K_{ip} + K_{ii}) \\ -\omega_3 R_f \end{pmatrix} s^2 + \omega_3 K_{ii}(H-1)s}$$

(23)

$$y_5 = L_f C_f$$
$$y_4 = C_f(R_f + \omega_3 L_f + K_{ip})$$
$$y_3 = c_f w_3(R_f + K_{ip} + y_3) + C_f K_{ii} + K_{ip} K_{vp}$$
$$y_2 = \omega_1 C_f K_{ii} + K_{ip} K_{vi} + K_{ii} K_{vp} + \omega_3 K_{ip} K_{vp}$$
$$y_1 = K_{ii} K_{vi} + \omega_3 (K_{ip} K_{vp} + K_{ip} K_{vi})$$
$$y_0 = \omega_3 K_{ii} K_{vi}$$

V. EVALUATION RESULTS

The system consists of single DG units with rated power of 30 kVA. At the load side, three CILs are implemented. CIL-1 is an 8 hp PMSM drive system interfaced to the micro-gird via back-to-back PWM voltage-sourced controlled converters; CIL-2 is a 5 kW linear load; CIL-3 is a 6 kW Non-linear load.

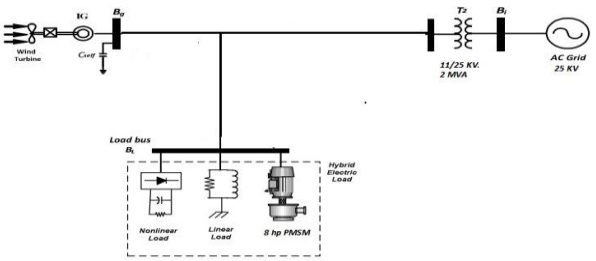

Fig. 5 AC Micro-grid connected to 11 KV Distribution System

A. *Simulation Result of Converter-Fed Ac Micro-Grid without Compensator*

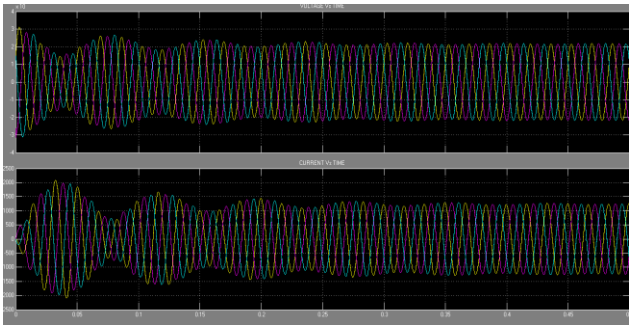

Fig 5.1 Voltage and current unbalance at grid side

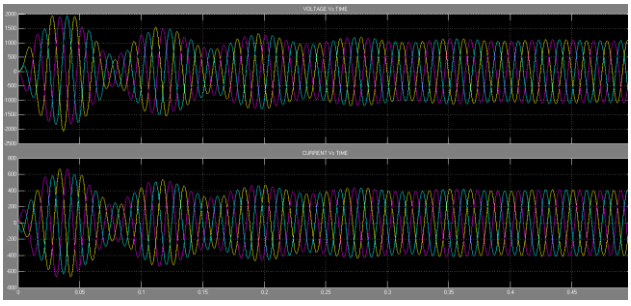

Fig 5.2 Voltage and current unbalance at Common AC Bus

It can be noted that the voltage unbalance and power factor reduction are obtained at loading conditions. When the AC Micro-grid operates parallel with utility grid supplying the load, however without any compensator associated with voltage source converter there has been voltage unbalance and power factor reduction due to the tightly regulated converter interfaced loads. The measured power factor in this scenario is 0.75.

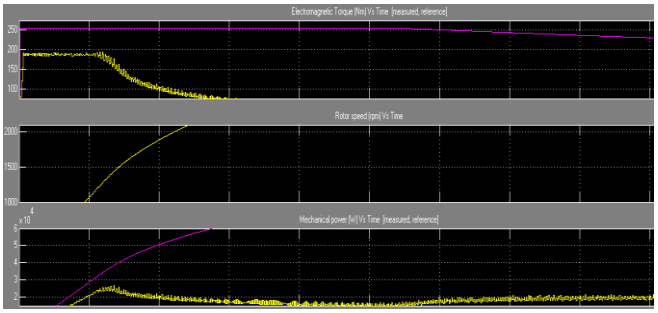

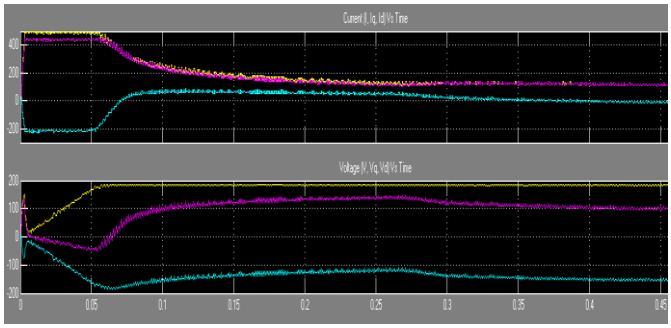

Fig 5.3 Permanent Magnet Synchronous Motor Output Without Compensator.

B. Simulation Result of Converter-Fed Ac Micro-Grid with Compensator

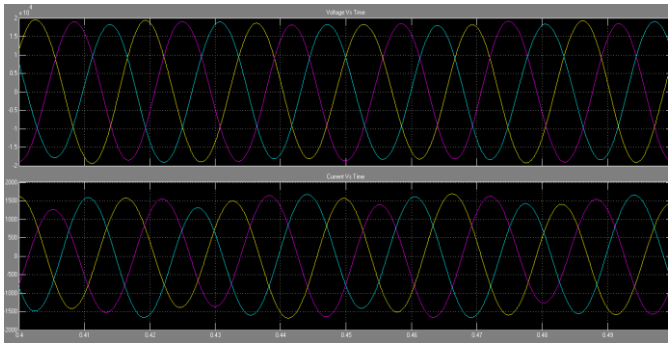

Fig 5.4 Voltage and current unbalance at grid side

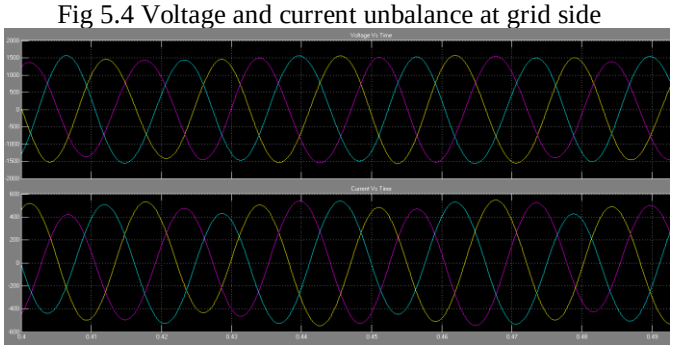

Fig 5.5 Voltage and current unbalance at common AC Bus

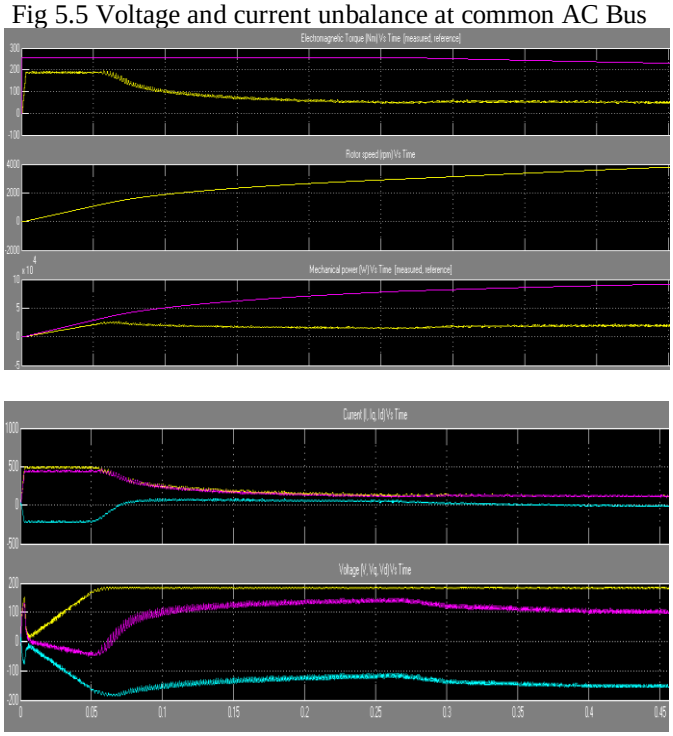

Fig 5.6 Permanent Magnet Synchronous Motor Output With Compensator.

VI. Conclusion

Active compensation techniques have been proposed to actively satisfy the Voltage unbalance from the VSI side. Compensated sources impedance and modified voltage tracking dynamics have been derived under the presence of the proposed active damping compensators to facilitate multi objective design of the active damping controllers with reduced interactions with existing converter control loops. Therefore, by effective use of compensator at voltage source converter, the voltage unbalance has been balanced and the respective power factor reduction has been improved. The proposed compensators have the following advantages:

1) They are linear, with simple design and implementation characteristics.

2) The power rating of the interfacing VSI with its filtering components are only required to design the compensator regardless of the terminated power electronic loads.

References

[1] Y. A.-R. I. Mohamed, H. Zeineldin, M. Salama, and R. Seethapathy, "Seamless formation and robust operation of distributed generation micro-grids via robust direct voltage vector control and optimized dynamic power sharing," IEEE Trans. Power Electron., vol. 27.

[2] D. Boroyevich, I. Cvetkovic, D. Dong, R. Burgos, F. Wang, and F.Lee, "Future electronic power distribution systems—a contemplative view,"in Proc. 2010 12th OPTIM Int. Conf., pp. 1369–1380.

[3] A. M. Rahimi and A. Emadi, "Active damping in DC/DC power electronic converters: A novel method to overcome the problems of constant power loads," IEEE Trans. Ind. Electron., vol. 56, no. 5, pp. 1428–1439, 2009.

[4] A. M. Rahimi, G. A. Williamson, and A. Emadi, "Loop-cancellation technique: A novel nonlinear feedback to overcome the destabilizing effect of constant-power loads," IEEE Trans. Veh. Technol., vol. 59,no. 2, pp. 650–661, Feb. 2010.

[5] A. Bin Jusoh, "The instability effect of constant power loads," in Proc. 2004 Natl. Power Energy Conf., pp. 175–179.

[6] X. Liu, A. J. Forsyth, and A. M. Cross, "Negative input-resistance compensator for a constant power load," IEEE Trans. Ind. Electron., vol.54, no. 6, pp. 3188–3196, 2007.

[7] P. Liutanakul, A.-. Awan, S. Pierfederici, B. Nahid-Mobarakeh, and F. Meibody-Tabar, "Linear stabilization of a DC bus supplying a constant power load: A general design approach," IEEE Trans. Power Electron., vol. 25, no. 2, pp. 475–488, 2010.

[8] X. Liu and A. J. Forsyth, "Comparative study of stabilizing controllers for brushless DC motor drive systems," Proc. 2005 IEEE IEMDC, pp. 1725–1731.

[9] A. Emadi, "Modeling of power electronic loads in AC distribution systems using the generalized state-space averaging method," IEEE Trans. Ind. Electron., vol. 51, no. 5, pp. 992–1000, 2004.

[10] S. D. Sudhoff, S. F. Glover, P. T. Lamm, D. H. Schmucker, and D. E. Delisle, "Admittance space stability analysis of power electronic systems," *IEEE Trans. Aerosp. Electron. Syst.*, vol. 36, no. 3, pp. 965–973, 2000.

[11] J. Sun, "Impedance-based stability criterion for grid-connected in verters," *IEEE Trans. Power Electron.*, vol. 26, no. 11, pp. 3075–3078, 2011.

[12] M. Cespedes, L. Xing, and J. Sun, "Constant-power-load system stabilization by passive damping," *IEEE Trans. Power Electron.*, vol. 26, no. 7, pp. 1832–1836, 2011.

[13] A. Kwasinski and C. Onwuchekwa, "Dynamic behavior and stabilization of dc micro-grids with instantaneous constant-power loads," *IEEE Trans. Power Electron.*, vol. 26, no. 3, pp. 822–834, 2011.

[14] W. Zhang, Y. Hou, X. Liu, and Y. Zhou, "Switched control of three-phase voltage source PWM rectifier under a wide-range rapidly varying active load," *IEEE Trans. Power Electron.*, vol. 27, no. 2, pp. 881–89.